

## Influence of natural clouds on the performance of solar cell systems in Iraq

Hiba Nadhim Ameen Al-Kaoaz, Omar Sharaf Al-deen Yehya Al-Yozbak

Department of Electrical Engineering, College of Engineering, University of Mosul, Mosul, Iraq

### Article Info

#### Article history:

Received Sep 4, 2022

Revised Dec 16, 2022

Accepted Jan 10, 2023

#### Keywords:

Energy  
Irradiation  
Partial shading  
Photovoltaic  
Weather condition

### ABSTRACT

Solar energy generated by photovoltaic (PV) technology can be supplied to standalone systems, as it combines efficiency and cost-effectiveness. However, this combination is achieved only after considering the effects of shading, which can significantly influence electrical output. The primary factor that influences the use of solar energy in electricity generation is irradiation. PV cells are significantly impacted by shading, where the output of the PV cell reduces in the presence of a shadow. In this study, the researchers have presented an experimental analysis of how shading affects two PV cells, using the series and parallel configurations. The experimental work is installed at the University of Mosul, Department of Electrical Engineering, Renewable Lab (Iraq). MATLAB was used to simulate, evaluate, and compare the results to understand the effects of shading on PV cell output. This research offers an analytical technique to determine the probable effects of Partial shadowing conditions on PV power generation. The results provide the effects of partial shadowing in an annual performance loss of  $\geq 10\text{--}30\%$ . The orientation of the PV panels' tilt angle has an impact on their output power. When the tilt angle deviates from its ideal value, the PV panel's output drops off substantially.

This is an open access article under the [CC BY-SA](https://creativecommons.org/licenses/by-sa/4.0/) license.



### Corresponding Author:

Omar Sharaf Al-deen Yehya Al-Yozbak

Department of Electrical Engineering, College of Engineering, University of Mosul

Mosul, Iraq

Email: o.yehya@uomosul.edu.iq

## 1. INTRODUCTION

Energy was a great discovery of human beings which made our life more and more comfortable [1]. Increasing consumption and demand for energy shows that energy will be one of the major problems in the world [2]. An alternative renewable energy source is the answer. In many nations, the production of electricity is increasingly dependent on renewable energy sources. Electricity is generated using a variety of renewable resources, including wind energy, solar energy, and geothermal energy. The best option for generating electricity in countries with high solar radiation intensity is solar energy [3]. Solar energy is described as energy produced by heat or sunlight [4]. Solar energy has tremendous potential to mitigate the adverse impact of fossil fuel utilization. Due to its accessibility throughout the globe, solar energy is regarded as one of the best sources of renewable energy [5]. The usage of renewable energies is prioritized in various regions in the world due to the pollution generated by fossil fuels. Solar energy is regarded as the most important form of energy, and is seen to be renewable, widely-distributed and does not harm the atmosphere.

The photovoltaic (PV) process can be described as a technological process where sunlight is converted to direct current (DC) [6]. To produce a PV system with the appropriate voltage and loading current capacity, numerous modules are coupled in the series and/or parallel configurations [7]–[11]. The higher efficiency of the solar energy technologies and declining investment costs have made electricity

generation from solar energy very popular in the past few years. The direct conversion of solar radiation energy to electrical energy by PV panels is well recognized. They do not contain any mechanical or moving components, which is the main perk of a PV system. However, they are influenced by several environmental conditions, like dust, dye, partial or total shading, among other elements. The PV panel efficiency is most strongly influenced by shade. The PV panels become less effective when they are covered by dust, clouds, or other obstructions [12], [13]. Shading the PV panels can prevent voltage drops at their terminals, which reduces the extracted power. Additionally, the unobstructed or clean PV panels are impacted by the shaded or dirty ones. Sometimes, since some PV systems or module components receive less intense sunlight due to clouds or the shadows created by neighboring trees, buildings, and other objects, a partially-shaded condition is unavoidable [14], [15]. It is well-known that partial shadowing causes a corresponding reduction in the output power of PV arrays. The characteristic curves of PV arrays were thought to be negatively impacted by partial shading (PS) [16]–[18].

A tool that predicts how PV generators will react to different weather scenarios is necessary for the design and study of PV modules. The electrical specifications of PV panels are often provided by the manufacturers under standard test conditions (STC), which include the solar radiation of  $1,000 \text{ W/m}^2$  and cell temperatures of  $25 \text{ }^\circ\text{C}$ . Many PV module models have been designed to describe how a PV module performs in various weather conditions [16], [19]. However, there is a need to experimentally investigate the validity of these models in predicting the performance of PV modules under different climatic conditions. However, there are some disadvantages to PV systems, such as high manufacturing cost, low power conversion efficiency of PV modules and extreme power degradation with varying impedance values. In addition, the PV system gives a naturally occurring nonlinear characteristic (V-I) which varies with temperature and radiation intensity [20]. In this paper, determined the effect of the cloud on the performance of the PV module. Although the presence of the cloud is statistical, conducting experiments for some days may allow one to have the presence of the cloud in one or two days, which enables him to identify the quantitative effect of the cloud on the panel function.

## 2. OVERVIEW OF THE CLIMATIC CONDITIONS IN IRAQ

The Mediterranean Sea has a considerable impact on Iraq's climate since it causes the climatic depression in the winter, which affects the temperature and precipitation patterns. The wintertime west winds that cause climatic depressions in the central and northern regions in Iraq, together with warm winter rains, also have an impact on the gulf. The four different seasons in Iraq, which have varying durations, exhibit a variety of climatic characteristics. Iraq has 2 major seasons, i.e., winter and summer, along with the shorter spring and autumn seasons. During the Iraqi Summer, which lasts from June to August, the sun is at approximately  $90^\circ$  in the northern hemisphere [21].

Between December and January, Iraq sees a normal winter season that is defined by two important changes: i) the temperature in Iraq drops significantly during the winter, with the central and northern regions occasionally experiencing winter nights with temperatures as low as zero. The monthly heat rate in Iraq lowers as one travels from the southern to the northern regions and ii) during the winter, the winds blow across the nation when a depression is seen in the Mediterranean Sea. The northwesterly and western winds originate in high-pressure regions and move to low-pressure regions.

The south-western winds only blow during thunderstorms or when there is a depression brought on by the north-western winds, whereas the north-western winds blow all year round. The wind usually comes from the east or north-east during the winter, which drastically decreases temperatures. Due to its climate and location, Iraq receives direct normal radiation that varies between  $1,800$  and  $2,390 \text{ kWh/m}^2/\text{year}$  [22]. Iraq thus has a lot of potential for producing electricity from solar radiation. Based on information provided by the solar electricity handbook [23]. In many locations across the world, including some in Iraq, Table 1 compares the amount of solar energy that can be captured when the sun's rays are incident on the horizontal, vertical, or optimally-inclined planes. Each and every city in Iraq had exceptional amounts of sun irradiation, as seen in Table 1. The amounts of sun irradiation on the horizontal, vertical, and best-inclined planes at the best angles are shown in Table 1 for a number of locations where solar thermal power plant (STPP) plants have been built around the world, including several spots in Iraq.

Iraq's geographic location is crucial since it facilitates the production of electricity, particularly when considering renewable energy sources. Research by Trieb [24], Iraq is situated in a region where the yearly average daily energy that is generated from global sun irradiation ranges from  $2,000$  to  $2,500 \text{ kWh/m}^2$ . Figure 1 displays typical and global solar distributions.

Table 1. Solar irradiation levels in few Iraqi cities

Location	Country	Irradiation on horizontal plane (Wh/m <sup>2</sup> /year)	Irradiation on vertical plane (Wh/m <sup>2</sup> /year)	Irradiation on inclined plane (Wh/m <sup>2</sup> /year)	Optimal Inclination
San Bernardino	USA	5294	3637.5	5875.8	56
Phoenix	USA	5280	3685.8	5895.8	57
Seville	Spain	4868.3	3443.3	5410.8	53
Badajoz	Spain	4705.8	3405	5268.3	51
New castle	Australia	4590	3154	5031	57
Abu Dhabi	UAE	5533.3	3186.6	5847.5	66
Cairo, Egypt	Egypt	5290	3227.5	5647.5	60
Mosul	Iraq	4841.6	3319.1	5319.1	54
Mosul	Iraq	5011.6	3227.5	54025	56
Al-Anbar	Iraq	5000	3136.66	5347.0	57
Karbala	Iraq	5104.16	3236.6	54925	57
An Nasiriya	Iraq	5129.16	3219.16	5505.8	59
Al-Basrah	Iraq	5035.8	3086.6	5276.66	60

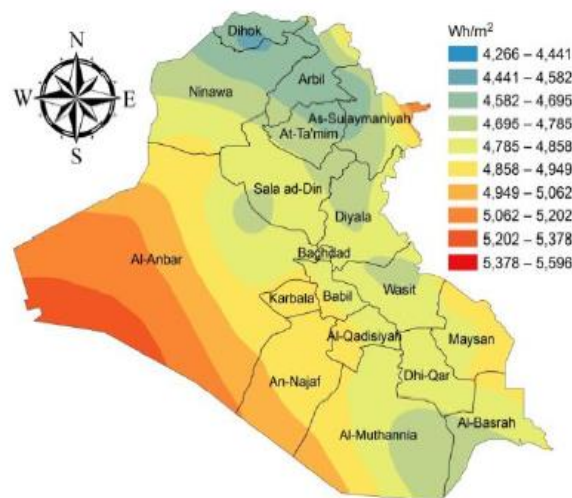


Figure 1. Iraq's direct and global solar irradiation [24]

### 3. SHADOW EFFECT

The shadow effect has great impact on the PV cell output. In several previous papers, the impact of shadow on PV cell was described [25], [26], here a very simple Simulink based design is presented to understand the shadow effect and to make it understandable to general people. People can easily see the effect of the shadow, where the connections are in series and where the connections are parallel. Shadow effects are categorized into two types, when the solar panel is covered in dust or any other solid particles, such as bird droppings, that partially or totally prevent solar irradiance from reaching the solar panel, this is referred to as static shading or hard shading. A thin coating of dirt accumulates on top of a solar panel when it is dusted, reducing the power output of the solar panel. If this layer becomes sufficiently thick, it will entirely prevent the panel from receiving any sunlight. Bird droppings are another factor in static or harsh shading. When an object prevents sunlight from reaching the solar panel, this is known as dynamic shading or soft shading. This object could be a stationary tree and structure. PS is another name for dynamic shading that covers a portion of the PV panel.

Since of how the sun's position varies during the day, this sort of shade is referred to be dynamic because the shadow constantly moves. The relative location of the sun changes as the earth rotates around its own axis, which alters the size and shape of the shade. Therefore, this sort of shade is least at noon (in some regions) when the sun is directly overhead the PV installation, and it increases at other times of dawn and nightfall. Some people also categorize the shadow effects in the same way but their basis is different from this work. Here 1000 W/m<sup>2</sup> is used as the margin between soft shadow and hard shadow. From 0 to 1,000 W/m<sup>2</sup> is called as soft shadow. The main effect of shadow is the reduction in irradiation value. When the obstacles block the light of the sun, the light cannot get to the PV cell directly and reduce the power of the light [27]–[29]. For the shadow effect the output of the series and parallel connection's PV cells is reduced [30], [31].

#### 4. THE TILT EFFECT

The solar angles (tilt and azimuth angles) can be used to pinpoint the sun's altitude in relation to any place on earth. The efficiency of PV panels is significantly influenced by their tilt angle. To achieve optimal power output, it is crucial to install the PV panels at the proper tilt angle for the site. PV panels are very effective when they are positioned in a perpendicular direction to the rays of the sun. Azimuth and tilt angles are shown in Figure 2. However, the position of the sun and its altitude change throughout the year. During the summer months, the altitude angle value at the highest point in the sun's path will be at its maximum, especially on 21<sup>st</sup> June; while it is the lowest during the winter months, particularly, on 21<sup>st</sup> December. The tilt-o-angle begins at 90°, during sunrise, and decreases until midday, when it reaches its lowest point, before increasing again to 90° at sunset. Every location has a distinctive tilt angle for different times of the year since the tilt angle is time- and place-dependent. The (1)-(7) can be used to determine the tilt angle for every location and time during the year [32].

$$AST = LST + \left( \frac{4min}{deg} \right) (LSTM - Long) + ET \quad (1)$$

Where AST is apparent solar time, LST is local standard time, and LSTM is local longitude

$$LSTM = 15^\circ \times \left( \frac{Long}{15^\circ} \right)_{round\ to\ integer} \quad (2)$$

Where long is longitude

$$ET = 9.87 \sin(2D) - 7.35 \cos(D) - 1.5 \sin(D) \quad (3)$$

$$D = \frac{360^\circ(n-81)}{365} \quad (4)$$

Where  $n$  is number of days until the required date

$$\text{The declination angle, } \delta = 23.45^\circ \sin \left[ \frac{n+284}{365} \right] \times 360 \quad (5)$$

$$\text{The hour angle, } H = \frac{\text{No of mins past midnight} \cdot AST - 720 \text{mins}}{4 \text{ mins/deg}} \quad (6)$$

$$\text{The tilt angle, } \theta_z = \cos^{-1}(\cos(Lat)\cos(\delta)\cos(H) + \sin(Lat)\sin(\delta)) \quad (7)$$

Where LAT is latitude

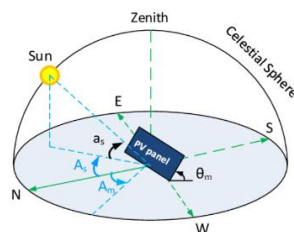


Figure 2. Solar tilt

#### 5. METHOD AND MATERIALS

Here the effect of the shadow on the PV cells is observed using Simulink model and practical model which would be understandable by everyone in this work is used as soft shadow. From the simulation circuit, the value of solar radiation was taken with the value of the cell current and cell voltage. In addition, the characteristics of the P-V were plotted, the values of the V-I characteristics of the cell were taken, and the effect of radiation on the cell current was also plotted. From the experimental circuit, the effect of the angle of inclination on the efficiency of the solar cell was taken, as the efficiency of the solar cell is affected by the angle of inclination. In addition, solar cells were connected to different loads.

These loads are either linear or non-linear, as the linear load consists only of resistance, while the non-linear load consists of resistance and inductance. The results were taken as represented by the value of the load current, voltage, real power, reactive power, power factor, and total harmonic distortion (THD) of voltage and current in the presence of the source. In addition, the results were taken with the battery for a linear load once and for a non-linear load again. Then the effect of PS was taken. Where PS of the cell was done in the horizontal direction once and in the vertical direction again as a representation of the effect of clouds on the efficiency of the solar cell.

**5.1. The PV simulation model**

Figure 3 illustrates how a typical residential PV system connected to the electrical utility grid operates, and show the effect of the irradiation on the dc current of the PV, and show the effects of partial shadow on the output power of the PV. The model was simulated by using MATLAB/Simulink. The grid is modeled using an ideal AC source of 240 Vrms. The residential load (240 W @ 240 Vrms).

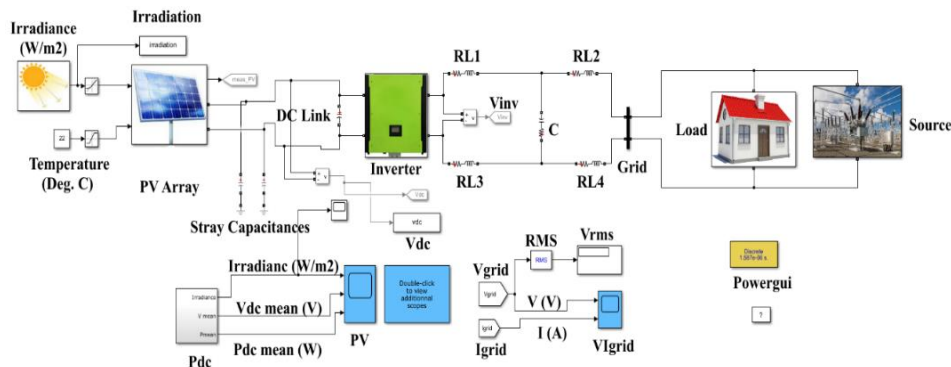


Figure 3. PV simulation model

**5.1.1. PV array**

The operations research experiment framework (OREX) model's implementation of the PV array consists of PV modules linked in parallel and series. You can enter variable data for temperature (input T in °C) and solar irradiance (input Ir in W/m<sup>2</sup>) using the PV array block's two input values. In the study's example, the PV array consists of a single string of two trina solar OREX PV modules that are wired in series. At a temperature of 22 °C and a sun radiation of 1,000 W/m<sup>2</sup>, this string produces 340.014 W. Two small capacitors connected to the positive and negative terminals of the PV array are used to represent the parasitic capacitance between the ground and PV modules. The properties of a PV array are shown in Figure 4.

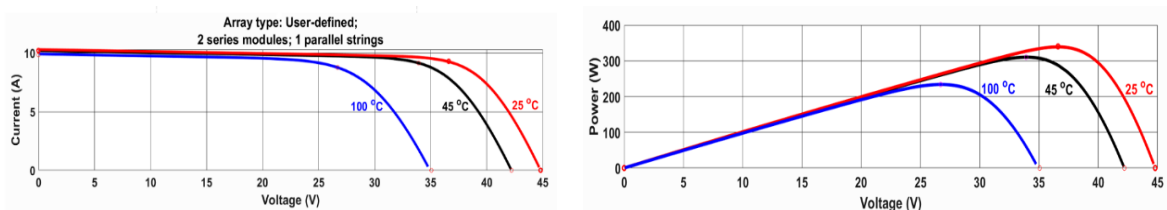


Figure 4. PV array characteristics

**5.1.2. DC/AC converter (one-phase)**

The inverter is modelled by a single-phase full-bridge insulated gate bipolar transistors (IGBT) module with pulse-width modulation control (H-bridge). As shown in Figure 5, the topology of a grid-side filter is seen to be the traditional LCL structure with an equal number of inductors that are placed on the line and neutral branches. Maximum power point tracking (MPPT) technology automatically adjusts the voltage direct current (VDC) reference signal of the inverter VDC regulator to generate a DC voltage that increases the power drawn from the PV string. Pulse width modulation (PWM) for generating the firing signals to IGBTs. where PWM is the inverters' most used approach. PWM is used to pulse-control the DC voltage,

turning it on and off. Each pulse's width is adjusted such that the overall electrical result resembles a sine wave. The majority of the inverter is made up of an easy H-bridge configuration. The circuit uses IGBT to build a single-phase H-bridge circuit.

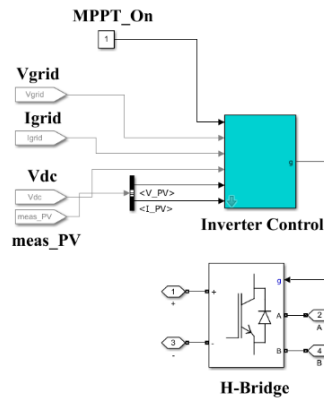


Figure 5. One-phase DC/AC converter model

**5.1.3. Inverter control**

The inverter control system includes 5 primary Simulink®-based subsystems: MPPT controller: the 'perturb and observe' process is necessary for the (MPPT) controller to function. To produce a DC voltage that will maximise the power extracted from the PV string, the MPPT technology automatically modifies the VDC reference signal of the inverter VDC regulator. Calculate the required Id (active current) reference for the power regulator when using a VDC regulator. Present-day regulator: the regulator determines the required reference voltage value for the inverter using the current references, i.e., Id and Iq (reactive current). The Iq reference's value was set to zero in the example above. Phase-locked loop (PLL) and measurements: required for voltage/current measurements and synchronization. IGBT firing signals are produced using the PWM generator, a technology that uses bipolar modulation. As seen in Figure 6, the PWM carrier frequency in the aforementioned case was adjusted to 3,150 Hz (63×50).

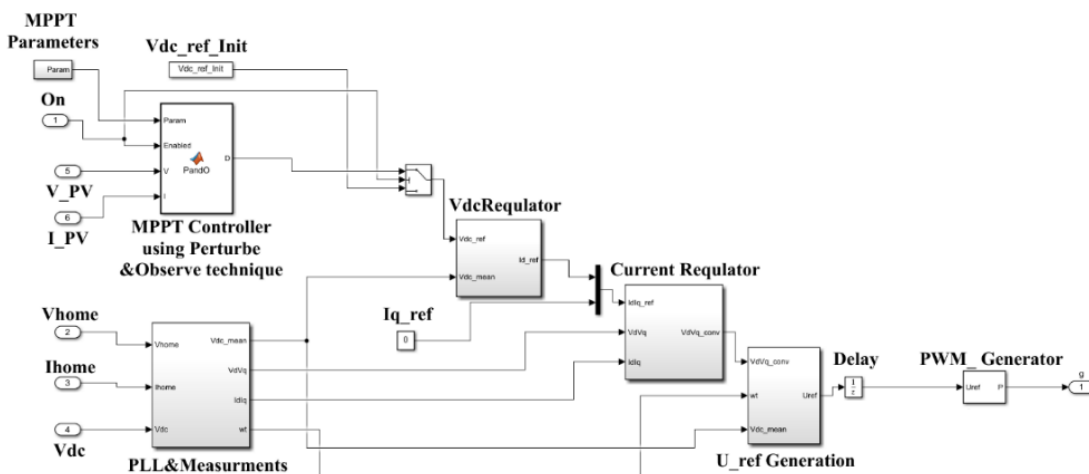


Figure 6. Inverter control model

**5.2. Outdoor experimental processes (solar panel components)**

An experimental bench was installed in the renewable lab in the Department of Electrical Engineering, University of Mosul, Iraq. Various array configurations that exhibit different behaviours under the PS conditions have been proposed to test PV system performance. The following components constitute the experimental solar panel.

### 5.2.1. Solar panel

Solar energy is utilized to generate electricity through the PV panels. PV panels are composed of many separate cells that are coupled together to generate power at a given voltage. PV panels are intrinsic DC gadgets. They need to be used with an inverter to generate AC. The PV panel is depicted in Figure 7 and is made up of 9 parallel cells in series and 4 series cells in series. Table 2 presents the characteristics of the PV panel.



Figure 7. PV panel

Table 2. PV characteristics

OREX future for energy	Monocrystalline photovoltaic modular
ITEM NO	AR-170 W
Rated maximum power	170 W
Power sorting	0 ~ +(0-5 W)
Voltage at Pmax (Vmp)	18.3 V
Current at Pmax (Imp)	9.29 A
Open-circuit voltage (Voc)	22.4 V
Short circuit current (Isc)	10.22 A
Maximum system voltage	1,000 V
Maximum series overcurrent protective device rating	15 A
Weight	11 kg
Dimensions	1480×680×35 mm
All technical standard test condition	
Safety application class	
Temperature coefficient (Pmax)	-0.37% °C
Temperature coefficient (Voc)	-0.29% °C
Temperature coefficient (Isc)	-0.05% °C
STC:1000 W/m <sup>2</sup> , AM 1.5, 25 °C	

### 5.2.2. Inverter

The inverter types free power, 1 Kw, 12 VDC was connected to the solar cell in order to convert the output of the PV to AC and prepare the loads from the PV when the supply from the utility was interrupted. This multi-purpose inverter charger combines the capabilities of an inverter, solar charger, and battery charger to provide uninterruptible power backup in a small, portable package. Its comprehensive LCD display offers user-configurable and convenient button operation, including allowable input voltage based on various applications, battery charging current, and priority for the AC/solar charger.

### 5.2.3. Battery

Use 150 Ah battery to supply the load when the utility and solar energy is not sufficient. Its life span is thus determined by the battery's design and quality. It is also affected by the battery's consumption and the appliance load on it. If your 150 Ah battery is fully charged, it should last for around 3 hours on a 400-watt bulb load. The backup will improve if the load or appliance wattage is lowered.

### 5.2.2. Loads

Linear and non-linear loads were used, their values ranged between 40 W-270 W. Several values were used with different scales. The readings of voltage, current, real and imaginary power, power factor, total harmonic distortion voltage (THDV), and THDI were used for all values of linear and non-plan loads, as shown in Figure 8, where the circuit in Figure 8 represents the experimental circle the work used in this work.



Figure 8. The whole practical circuit

## 6. RESULTS AND DISCUSSION

After completing the modeling of the working circuit and conducting the practical experiment, the effect of PS on the current of the PV cell was taken at rates (0%, 25%, 50%, and 100%). The effect of radiation on the voltage of the PV cell was taken, and the values for the characteristics of the PV cell were taken from the modeling circuit. As for the practical results, the effect of the angle of inclination was taken, where the angle of inclination was changed by values (0, 30°, 45°, 60°, and 85°). The effect of the linear load was also taken with the presence of the source once and the presence of the battery again and at an angle of inclination of 30°, because this is the angle at which the cell current is the highest possible. The effect of the non-linear load was taken with the source once and with the battery again and at the same angle, i.e. 30°. The effect of PS (soft shading) was taken in this work on the current of the PV cell in percentages (0%, 25%, 50%, and 100%) Taking the PS effect in the horizontal direction once and in the vertical direction again.

### 6.1. Effect of the irradiance on the PV current

After performing the modeling circuit, the radiation was changed and the cell current was measured for each value of solar radiation. It was noted that the increase in solar radiation leads to an increase in the cell current until we reach the radiation that reaches the greatest value. The cell current is at its maximum value of 9.29 A, as shown in Figure 9. The effect of solar radiation values on the cell current was also taken at different rates (0%, 25%, 50%, and 100%), where we notice that the less solar radiation, the lower the cell current, meaning that when PS increases, the cell current will decrease. That is, there is an inverse proportion between PS and cell current, as shown in Table 3. On Tuesday, practical readings were obtained in the University of Mosul's, Department of electrical engineering labs, April 19, 2022, and the weather was partly cloudy, which is the nature of Iraq's climate in the spring, where some days are partly cloudy while others are sunny. These readings were taken at one o'clock Ten in the morning the temperature was 22 °C.

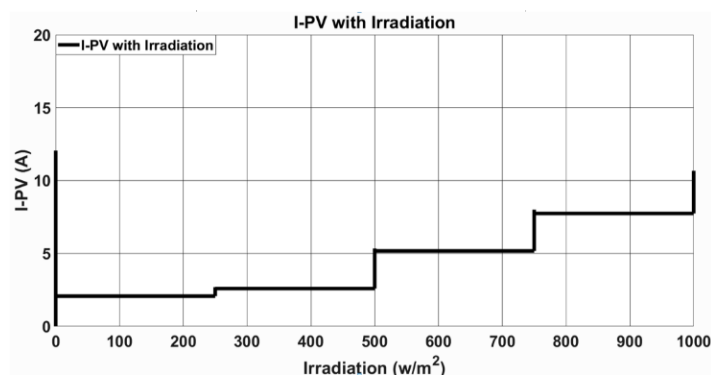


Figure 9. I-PV with irradiation

Table 3. DC current with partial shadow

Irradiance (W/m <sup>2</sup> )	Partial shadow (%)	I <sub>DC</sub> (A)
1,000	0	10.44549965
750	25	7.898006754
500	50	5.28701052
250	75	2.588009688
0	100	2.070978515



## 6.2. PV characteristics

The values for the characteristics of the solar cell were taken from the modeling circuit, where the value of current and power was taken with the cell voltage as shown in Table 4. Where it is noted that when the voltage increases, the output capacity of the PV increases, i.e. the proportionality is direct. Until the power reaches the value of MMPT, where the power begins to decrease until it reaches the value of zero. In this case, the proportionality becomes inverse between the output capacity of the PV and the voltage, while it is noted that when the value of the voltage increases, the current of the PV decreases until it reaches a value of zero, i.e. the inverse proportion between the voltage and the current.

Table 4. PV-characteristics from simulation model

V- PV (V)	Power-PV (W)	I-PV (A)
5	49.3	10.209
10	101.5	10.12
15	151.3	10.04
20	199.48	9.95
25	247.6	9.87
30	293.8	9.78
35	334.04	9.53
36.6	340.014	9.29
40	293.64	7.33
45	0	0

## 6.3. Effect of tilt angle

The readings were taken at different angles ( $0^\circ$ ,  $30^\circ$ ,  $45^\circ$ ,  $60^\circ$ , and  $85^\circ$ ) for tilting the solar cell. It affects the cell current where the cell current is directly proportional to the incident solar radiation and inversely proportional to the angle of inclination of the cell. Where notice that the greater the angle of inclination of the solar cell, the lower the current of the solar cell, and therefore this leads to a decrease in the output capacity of the cell and thus an increase in losses as shown in the results in Table 5 and Figure 10.

Table 5. DC current with angle

Angle (degree)	I-DC (A)
0	5.69
30	5.88
45	5.75
60	5.15
85	4.03

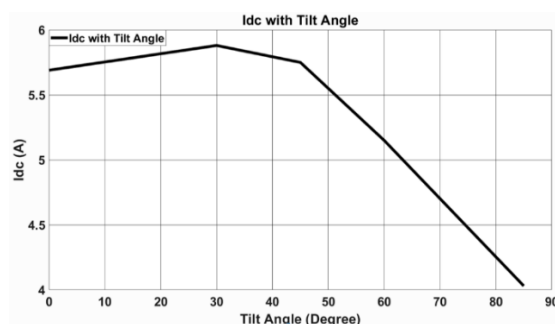


Figure 10. Idc with tilt angle

## 6.4. The effect of linear load in the presence of the source

After fixing the angle of inclination of the solar cell at  $30^\circ$ , because the cell current at this angle is as high as possible. The readings were taken in the presence of the source of the equipment, where the readings of the real and imaginary capacity. Power factor, current, voltage, THDV, THDI were taken for different values of linear loads and as shown in Table 6. It is noticed that when the load is increased, the load current increases and the real and reactive power also increases with the increase in the load. While THDV, THDI, power factor, and voltage remain at a constant value despite the increase in the load as shown in Figures 11 and 12.

Table 6. Active and reactive power with resistive load at  $\alpha=30^\circ$  from the supply

Load	$I_{AC}$ (A)	$V_{AC}$ (V)	P (W)	Q (VAR)	P.F	THD <sub>V</sub>	THD <sub>I</sub>
1	0.2	232	41.7	1.4	0.999	3.7	3.5
2	0.4	232	83	2.7	0.999	3.7	3.5
3	0.5	232	124	3.4	0.999	3.7	3.5
4	0.7	232	164	4.7	0.999	3.7	3.5
5	0.9	232	205	5.3	0.999	3.7	3.5

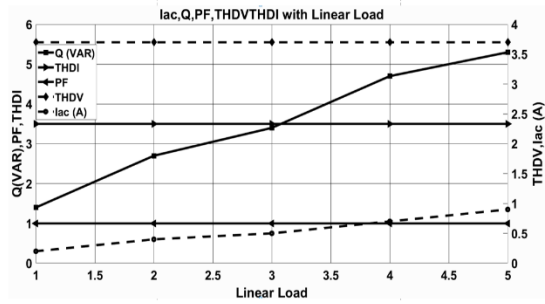


Figure 11.  $I_{ac}$ , Q, PF, THDV, THDI with linear load in the presence of the source

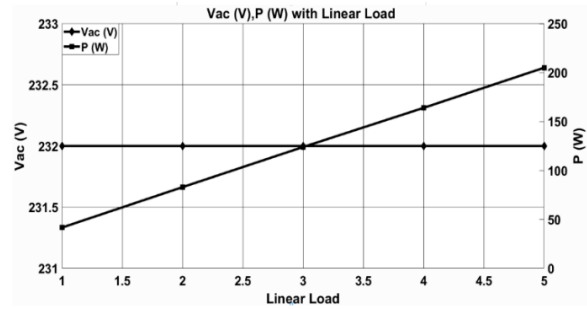


Figure 12.  $V_{ac}$ , P with linear load in the presence of the source

**6.5. The impact of nonlinear load with the source present**

After fixing the angle of inclination of the solar cell at  $30^\circ$ , because the current of the cell at this angle is the highest possible, the readings were taken in the presence of the source of the equipment. Where the readings of the real and imaginary capacity, power factor, current, voltage, THDV, THDI were taken for different values of non-linear loads and as shown in Table 7. It is noticed that when the load is increased, the load current increases by a greater percentage than the case of the linear load, and the real and reactive power also increases with the increase in the load as shown in Figures 13 and 14.

Table 7. Active and reactive power with RL load at  $\alpha=30^\circ$  from the supply

Load	$I_{AC}$ (A)	$V_{AC}$ (V)	P (W)	Q (VAR)	P.F	THD <sub>V</sub>	THD <sub>I</sub>
1	0.8	231	83	159	0.46	3.6	16.8
2	0.9	231	126	157	0.62	3.7	14.8
3	1	231	167	155	0.73	3.7	12.7
4	1.1	231	209	154	0.8	3.7	11
5	1.3	231	249	153	0.853	3.7	9.7
6	1.4	231	290	150	0.887	3.7	8.7

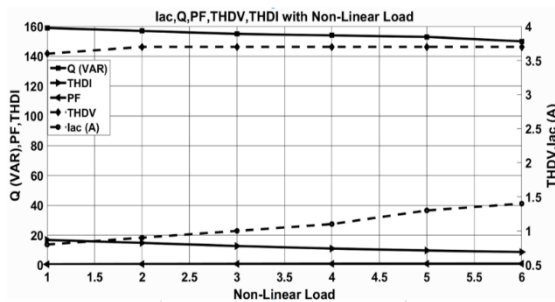


Figure 13.  $I_{ac}$ , Q, PF, THDV, THDI with non-linear load in the presence of the source

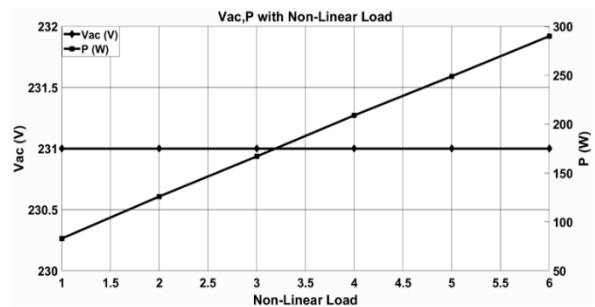


Figure 14.  $V_{ac}$ , P with non-linear load in the presence of the source

**6.6. Effect of a linear load when a battery is present**

After fixing the angle of inclination of the solar cell at  $30^\circ$ , because the current of the cell at this angle is as high as possible, the readings were taken with the battery for processing. Where the readings of

the real and imaginary capacity, power factor, current, voltage, THDV, THDI were taken for different values of linear loads and as shown in Table 8. It is noticed that when the load increases, the load current decreases, and the real and reactive power increases with the increase in the load. Also, the THDI increases by keeping the THDV, the voltage, and the power factor at a constant value despite the increase in the load as shown in Figures 15 and 16.

Table 8. Active and reactive power with resistive load at  $\alpha=30^\circ$  from the battery

Load	$I_{AC}(A)$	$V_{AC}(V)$	P (W)	Q (VAR)	P.F	THDV <sub>v</sub>	THDI <sub>t</sub>
1	229	0.2	40	3.4	0.999	34	35
2	229	0.4	80	6.5	0.999	34	33
3	226	0.5	119	9.6	0.999	34	34
4	226	0.7	158	13	0.999	34	34
5	224	0.9	200	17	0.999	34	34

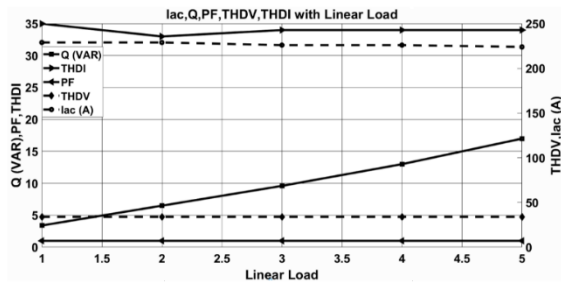


Figure 15. Iac, Q, PF, THDV, THDI with linear load in the presence of the battery

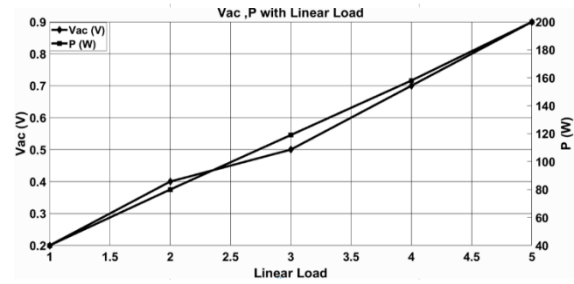


Figure 16. Vac, P with linear load in the presence of the battery

**6.7. The effect of a non-linear load in the presence of the battery**

After fixing the angle of inclination of the solar cell at  $30^\circ$ , because the current of the cell at this angle is the highest possible, the readings were taken with the battery for processing. Where the readings of the real and imaginary capacity, power factor, current, voltage, THDV, THDI were taken for different values of non-linear loads and as shown in Table 9. It is noticed that when the load is increased, the load current increases by a greater percentage than the case of linear load, and the real and reactive power also increases with the increase in the load as shown in Figures 17 and 18.

Table 9. Active and reactive power with RL load at  $\alpha=30^\circ$  from the battery

Load	$I_{AC}(A)$	$V_{AC}(V)$	P (W)	Q (VAR)	P.F	THDV <sub>v</sub>	THDI <sub>t</sub>
1	230	0.7	70	133	0.46	34	13.5
2	228	0.7	110	128	0.65	34	16.9
3	227	0.9	149	125	0.766	35	20
4	225	1	187	123	0.83	33	22
5	227	1.2	230	129	0.87	30.7	22.3
6	226	1.4	273	134	0.89	27	22

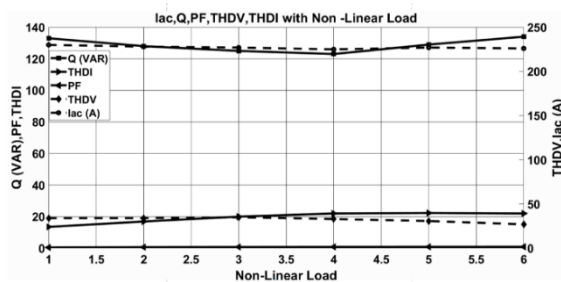


Figure 17. Iac, Q, PF, THDV, THDI with non -linear load in the presence of the battery

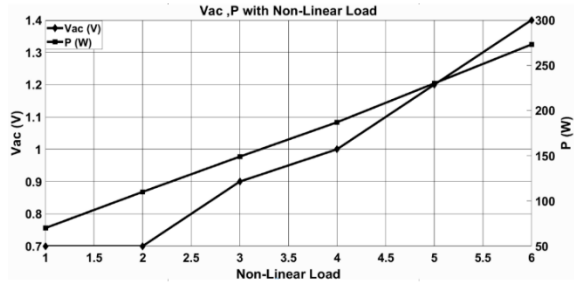


Figure 18. Vac, P with non -linear load in the presence of the battery

### 6.8. Partial shading effect (horizontal-position)

PS was done in the horizontal direction as shown in the Figure 19, and the cell current was measured at different percentages of PS (0%, 25%, 50%, and 100%). This action is similar to the cloud when it moves over the solar cell, causing PS of the cell and thus a decrease in current. This means that the current of the cell is inversely proportional to the percentage of PS of the cell as shown in Table 10 and Figure 19.

Table 10. Idc with horizontal partial variations

Partial horizontal variations (%)	$I_{DC}$ (A)
0	6.5
25	6.1
50	5
75	3.2
100	0.4

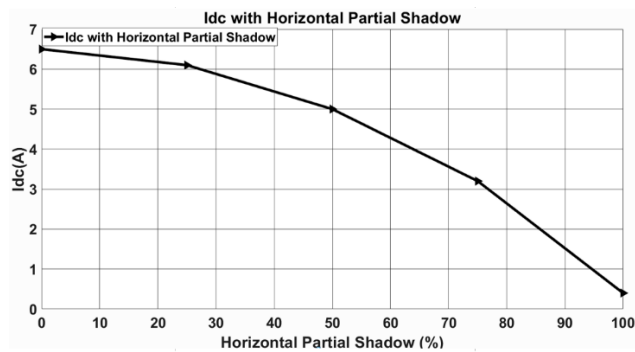


Figure 19. Idc with horizontal partial shadow

### 6.9. Parallel effect (vertical-position)

PS was done in the vertical direction and as shown in the Figure 20, and the cell current was measured at different percentages of PS (0%, 25%, 50%, 100%). This action is similar to the cloud when it moves over the solar cell, causing PS of the cell and consequently the current decrease. This means that the current of the cell is inversely proportional to the percentage of PS of the cell as shown in Table 11 and Figure 20.

Table 11. I dc with vertical partial variations

Partial vertical variations (%)	$I_{DC}$ (A)
0	6.5
25	6.1
50	4.8
75	2.6
100	0.49

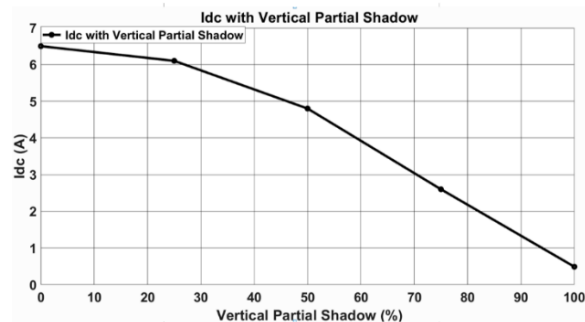


Figure 20. Idc with vertical partial shadow

## 7. CONCLUSION

This paper presents the effects of PS with the PV properties of the PV array. Simulations were performed in a MATLAB environment which gives a good understanding of the effect of PS on the PV (matrix) system. The effect of the angle of inclination on the output of the PV cell was practically studied by changing the angle with different values (0°, 30°, 45°, 60°, and 85°). From the results of the research it can be concluded that: The orientation of the PV panels' tilt angle has an impact on their output power. The PV panels' maximum output was observed at the project's optimal tilt angle of 30°, which meant that the sun's beams were perpendicular to the PV panel. When the tilt angle deviates from its ideal value, the PV panel's output drops precipitously (maintained at 30° in this study), and the output declines continually the more the tilt angle deviates. Partial shadowing poses a serious threat to PV systems. The results showed that the effects of the non-linear load on the PV cell are higher than the linear loads. The results showed that the effects of the non-linear load on the PV cell are higher than the linear loads. PS can significantly decrease the solar system's maximum power. Depending on the weight and patterns of the partial shade, the ability of the PV panels can fluctuate.

## ACKNOWLEDGEMENTS

The authors would like to thank University of Mosul, College of Engineering, Department of Electrical Engineering, for the support given during this work.




## REFERENCES

- [1] A. Malviya and P. P. Solanki, "Photogalvanics: a sustainable and promising device for solar energy conversion and storage," *Renewable and Sustainable Energy Reviews*, vol. 59, pp. 662–691, 2016, doi: 10.1016/j.rser.2015.12.295.
- [2] H. B. Khalil and S. J. H. Zaidi, "Energy crisis and potential of solar energy in Pakistan," *Renewable and Sustainable Energy Reviews*, vol. 31, pp. 194–201, 2014, doi: 10.1016/j.rser.2013.11.023.
- [3] A. Bouraiou, M. Hamouda, A. Chaker, M. Sadok, M. Mostefaoui, and S. Lachtar, "Modeling and simulation of photovoltaic module and array based on one and two diode model using MATLAB/Simulink," *Energy Procedia*, vol. 74, pp. 864–877, Aug. 2015, doi: 10.1016/j.egypro.2015.07.822.
- [4] M. K. Farooq and S. Kumar, "An assessment of renewable energy potential for electricity generation in Pakistan," *Renewable and Sustainable Energy Reviews*, vol. 20, pp. 240–254, 2013, doi: 10.1016/j.rser.2012.09.042.
- [5] M. Sabzpooshani and K. Mohammadi, "Establishing new empirical models for predicting monthly mean horizontal diffuse solar radiation in city of Isfahan, Iran," *Energy*, vol. 69, pp. 571–577, 2014, doi: 10.1016/j.energy.2014.03.051.
- [6] A. B. Jemaa, S. Rafa, N. Essounbouli, A. Hamzaoui, F. Hnaïen, and F. Yalaoui, "Estimation of global solar radiation using three simple methods," *Energy Procedia*, vol. 42, pp. 406–415, 2013, doi: 10.1016/j.egypro.2013.11.041.
- [7] E. Karatepe, T. Hiyama, M. Boztepe, and M. Çolak, "Voltage based power compensation system for photovoltaic generation system under partially shaded insolation conditions," *Energy Conversion and Management*, vol. 49, no. 8, pp. 2307–2316, 2008, doi: 10.1016/j.enconman.2008.01.012.
- [8] S. Lalouni and D. Rekioua, "Modeling and simulation of a photovoltaic system using fuzzy logic controller," in *2009 Second International Conference on Developments in eSystems Engineering*, 2009, pp. 23–28, doi: 10.1109/DeSE.2009.17.
- [9] N. Hamrouni, M. Jraïdi, and A. Chérif, "Theoretical and experimental analysis of the behaviour of a photovoltaic pumping system," *Solar Energy*, vol. 83, no. 8, pp. 1335–1344, 2009, doi: 10.1016/j.solener.2009.03.006.
- [10] A. Ubisse and A. Sebitosi, "A new topology to mitigate the effect of shading for small photovoltaic installations in rural sub-Saharan Africa," *Energy Conversion and Management*, vol. 50, no. 7, pp. 1797–1801, 2009, doi: 10.1016/j.enconman.2009.03.016.
- [11] S. O. -Amrouche, D. Rekioua, and A. Hamidat, "Modelling photovoltaic water pumping systems and evaluation of their CO2 emissions mitigation potential," *Applied Energy*, vol. 87, no. 11, pp. 3451–3459, 2010, doi: 10.1016/j.apenergy.2010.05.021.
- [12] K. Brecl and M. Topič, "Self-shading losses of fixed free-standing PV arrays," *Renewable Energy*, vol. 36, no. 11, pp. 3211–3216, 2011, doi: 10.1016/j.renene.2011.03.011.
- [13] S. Ghazi and K. Ip, "The effect of weather conditions on the efficiency of PV panels in the southeast of UK," *Renewable Energy*, vol. 69, pp. 50–59, 2014, doi: 10.1016/j.renene.2014.03.018.
- [14] A. Bidram, A. Davoudi, and R. S. Balog, "Control and circuit techniques to mitigate partial shading effects in photovoltaic arrays," *IEEE Journal of Photovoltaics*, vol. 2, no. 4, pp. 532–546, 2012, doi: 10.1109/JPHOTOV.2012.2202879.
- [15] Y. -H. Liu, S. -C. Huang, J. -W. Huang, and W. -C. Liang, "A particle swarm optimization-based maximum power point tracking algorithm for PV systems operating under partially shaded conditions," *IEEE Transactions on Energy Conversion*, vol. 27, no. 4, pp. 1027–1035, 2012, doi: 10.1109/TEC.2012.2219533.
- [16] M. Seyedmahmoudian *et al.*, "State of the art artificial intelligence-based MPPT techniques for mitigating partial shading effects on PV systems—a review," *Renewable and Sustainable Energy Reviews*, vol. 64, pp. 435–455, 2016, doi: 10.1016/j.rser.2016.06.053.
- [17] X. Fan, F. Deng, and J. Chen, "Voltage band analysis for maximum power point tracking of stand-alone PV systems," *Solar Energy*, vol. 144, pp. 221–231, 2017, doi: 10.1016/j.solener.2017.01.032.
- [18] R. Ahmad, A. F. Murtaza, H. A. Sher, U. T. Shami, and S. Olalekan, "An analytical approach to study partial shading effects on PV array supported by literature," *Renewable and Sustainable Energy Reviews*, vol. 74, pp. 721–732, 2017, doi: 10.1016/j.rser.2017.02.078.
- [19] R. P. Vengatesh and S. E. Rajan, "Investigation of cloudless solar radiation with PV module employing MATLAB-Simulink," in *2011 International Conference on Emerging Trends in Electrical and Computer Technology*, 2011, pp. 141–147, doi: 10.1109/ICETECT.2011.5760106.
- [20] R. Kerid and Y. Bounnah, "Modeling and parameter estimation of solar photovoltaic based MPPT control using EKF to maximize efficiency," *Bulletin of Electrical Engineering and Informatics*, vol. 11, no. 5, pp. 2491–2499, 2022, doi:




- 10.11591/eei.v11i5.3782.
- [21] O. S. A.-D. A.-Yozbakly and S. I. Khalel, "The future of renewable energy in Iraq: potential and challenges," *Indonesian Journal of Electrical Engineering and Informatics (IJEI)*, vol. 10, no. 2, pp. 237–291, May 2022, doi: 10.52549/ijeel.v10i2.3756.
- [22] J. Burgermeister, "Iraq looks to solar energy to help rebuild its economy," *Renewable Energy World*, 2009. <https://www.renewableenergyworld.com/storage/iraq-looks-to-solar-energy-to-help-rebuild-its-economy/#gref> (accessed Jan. 10, 2019).
- [23] M. Boxwell, "A simple, practical guide to solar energy--designing and installing solar photovoltaic systems," in *The Solar Electricity Handbook*, Coventry, England: Greenstream Publishing, 2017.
- [24] F. Trieb, "Concentrating solar power for the mediterranean region," Germany, 2005.
- [25] D. Sera, R. Teodorescu, and P. Rodriguez, "PV panel model based on datasheet values," in *2007 IEEE International Symposium on Industrial Electronics*, 2007, pp. 2392–2396, doi: 10.1109/ISIE.2007.4374981.
- [26] A. A. E. Tayyan, "A simple method to extract the parameters of the single-diode model of a PV system," *Turkish Journal of Physics*, vol. 37, no. 1, pp. 121–131, 2013, doi: 10.3906/fiz-1206-4.
- [27] R. Chenni, M. Makhlof, T. Kerbache, and A. Bouzid, "A detailed modeling method for photovoltaic cells," *Energy*, vol. 32, no. 9, pp. 1724–1730, 2007, doi: 10.1016/j.energy.2006.12.006.
- [28] S. Lineykin, M. Averbukh, and A. Kuperman, "Five-parameter model of photovoltaic cell based on STC data and dimensionless," in *2012 IEEE 27th Convention of Electrical and Electronics Engineers in Israel*, 2012, pp. 1–5, doi: 10.1109/EEEL.2012.6377079.
- [29] A. A. E. Tayyan, "PV system behavior based on datasheet," *Journal of Electron Devices*, vol. 9, pp. 335–341, 2011.
- [30] I. R. Balasubramanian, S. Ilango Ganesan, and N. Chilakapati, "Impact of partial shading on the output power of PV systems under partial shading conditions," *IET Power Electronics*, vol. 7, no. 3, pp. 657–666, 2014, doi: 10.1049/iet-pel.2013.0143.
- [31] D. Sera and Y. Baghzouz, "On the impact of partial shading on PV output power," in *International Conference on Renewable Energy Sources*, 2008, pp. 1–6.
- [32] S. J. M. Shareef, "The impact of tilt angle on photovoltaic panel output," *ZANCO Journal of Pure and Applied Sciences*, vol. 29, no. 5, pp. 112–118, 2017, doi: 10.21271/ZJPAS.29.5.12.

## BIOGRAPHIES OF AUTHORS



**Hiba Nadhim Ameen Al-Kaoaz**    she obtained her Bachelor of Science (BSc) in Electrical Engineering in 2002 from Department of Electrical Engineering, College of Engineering, University of Mosul, Iraq. Then she was appointed as an assistant engineer in the same mentioned department in 2003. After that, she got M.Sc in "Small signal stability analysis of a power system using wavelets", 2009 from the same mentioned department as well. Upon her graduation, she was appointed as teaching staff (assistant lecturer) in Department of Electrical Engineering, College of Engineering, University of Mosul. Now, she is Ph.D student in Department of Electrical Engineering, College of Engineering, and University of Mosul. The subjects for interest, renewable energy fields associated with the smart grid, power systems, and electrical machines. She can be contacted at email: hkaoaz@uomosul.edu.iq.



**Omar Sharaf Al-deen Yehya Al-Yozbakly**    he obtained his Bachelor of Science (B.Sc) in Electrical Engineering in 2001 from Department of Electrical Engineering, College of Engineering, University of Mosul, Iraq. Then he was appointed as an assistant engineer in the same mentioned department. After that, he got MSc in "Overcome the effect of critical distance in XLPE high voltage cables by inductive shunt compensator", 2008 from the same mentioned department as well. Upon his graduation, he was appointed as teaching staff (assistant lecturer) in Department of Electrical Engineering, College of Engineering, University of Mosul. In 2012, he obtained the scientific title (lecturer) and the Ph.D. degree in the Department of Electrical and Electronic Engineering, Faculty of Engineering, University Putra Malaysia in 2017. Since 2014, he was a member of the Centre for Electromagnetic and lightning protection research (CELP). Now, he is Assistant Professor at Department of Electrical Engineering, College of Engineering, University of Mosul. The subjects for interest, renewable energy fields associated with the smart grid, thermal modeling transformer design, and electrical machines. He can be contacted at email: o.yehya@uomosul.edu.iq.